Journal of Colloid and Interface Science **233,** 38–49 (2001)
doi:10.1006/jcis.2000.7227, available online at http://www.idealibrary.com on IDEAL®

Uranium(VI) Sorption Complexes on Montmorillonite as a Function of Solution Chemistry[1]

Catherine J. Chisholm-Brause,*[,2] John M. Berg,† Robert A. Matzner,‡ and David E. Morris§[,2]

*School of Marine Science, College of William and Mary, VIMS, Gloucester Point, Virginia 23062; †Nuclear Materials Technology Division and §Chemistry Division, MS J514, Los Alamos National Laboratory, Los Alamos, New Mexico 87545; and ‡United States Environmental Protection Agency, Washington, DC 20460

Received November 16, 1999; revised August 7, 2000

We have investigated the effect of changes in solution chemistry on the nature of uranyl sorption complexes on montmorillonite (SAz-1) at different surface coverages (1.43–53.6 μmol/g). Uranyl uptake onto SAz-1 between pH 3 and 7 was determined in both titration and batch-mode experiments. These pH values result in solutions that contain a range of monomeric and oligomeric aqueous uranyl species. Continuous-wave and time-resolved emission spectroscopies were used to investigate the nature of U(VI) sorbed to SAz-1. A discrete set of uranyl surface complexes has been identified over a wide range of pH values at these low to moderate coverages. For all samples, two surface complexes are detected with spectral characteristics commensurate with an inner-sphere complex and an exchange-site complex; the relative abundance of these two species is similar over these pH values at low coverage (1.43–2.00 μmol/g). In addition, surface species having spectra consistent with polymeric hydroxide-like sorption complexes form at the moderate coverages (~34–54 μmol/g), increasing in abundance as the capacity of the amphoteric surface sites is exceeded. Furthermore, a species with spectral characteristics anticipated for an outer-sphere surface complex is observed for wet paste samples at low pH (3.7–4.4) and both low (~2 μmol/g) and moderate (~40 μmol/g) coverage. There are only subtle differences in the nature of sorption complexes formed at different pH values but similar coverages, despite markedly different uranyl speciation in solution. These results indicate that the speciation in the solution has minimal influence on the nature of the sorption complex under these experimental conditions. The primary control on the nature and abundance of the different uranyl sorption complexes appears to be the relative abundance and reactivity of the different sorption sites.

Key Words: **uranium; sorption; clays; montmorillonite; emission spectroscopy; speciation; surface complexation.**

INTRODUCTION

Environmental contaminant releases that contain uranium are among the more serious problems that must be confronted by restoration programs. For example, uranium has been identified in complex contaminant mixtures at 12 U.S. Department of Energy facilities at concentration levels approaching 16,000 ppm in soils and sediments (1). Uranium mill tailings have also produced soil and mine-water contamination plumes having very high dissolved and solid uranium concentrations at pH values approaching 2.5 (2, 3). To assess the risk of surface and subsurface transport and facilitate restoration, information concerning the speciation of uranium in soils and groundwaters is needed. Under oxidizing conditions, dissolved uranium is predominantly in the U(VI) (uranyl) form (4, 5) and is potentially quite mobile in the environment. However, uranyl has been shown to strongly sorb to many soil constituents including clay minerals (6–13) and metal oxides (14–22) under appropriate chemical conditions, thereby affording a mechanism to retard its movement. In this study, we have investigated the effect of changes in solution chemistry and surface coverage on the nature of uranyl sorption complexes on montmorillonite, a common soil clay mineral.

Many factors have a bearing on the sorption of metal-ion species on clay minerals. In particular, metal-ion uptake behavior may vary as a function of pH, background electrolyte concentration, and surface coverage. Uranyl solution species become increasingly hydrolyzed and polymerized with increasing pH (5). Thus, changes in the extent of uranyl sorption and the nature of the sorption complex(es) with pH may reflect the sorption of different aqueous uranyl solution species. Alternatively, the distribution and reactivity of surface sites as a function of pH and background electrolyte may influence the distribution and nature of the uranyl surface complexes. Two broad classes of sorption processes are thought to occur on clays: exchange to fixed-charge sites located on the basal planes and sorption to amphoteric surface sites predominantly located at the edges of clay crystallites (23–26).

Exchange processes are thought to be generally independent of pH whereas adsorption to edge sites may be strongly pH-dependent due to the pH dependence of the formation of

[1] The U.S. Government's right to retain a nonexclusive royalty-free license in and to the copyright covering this paper, for governmental purposes, is acknowledged.

[2] To whom correspondence should be addressed. E-mail: cbrause@vims.edu; demorris@lanl.gov.

0021-9797/01 $35.00

amphoteric surface sites and the surface complexation reactions. Thus, formation of multiple sorption complexes may reflect bonding to distinct surface sites as a function of pH. In addition, exchange reactions are suppressed by relatively high levels of background electrolyte. Uranyl uptake by smectites has been successfully modeled as predominantly exchange at low background electrolyte solution concentrations and low pH and predominantly adsorption to amphoteric edge sites at high background electrolyte concentrations and/or higher pH values (10–12). Finally, surface coverage may influence the number and nature of the sorption complexes in several ways. Polymerization at the surface may be promoted at higher surface coverages even if the sorbing species is monomeric (27–30). Furthermore, the number of different sites may be limited; e.g., amphoteric edge sites constitute ≈5 to 20% of the total measured sorption capacity of smectites, and above this coverage occupancy of the basal-plane exchange sites and/or surface polymerization processes may be required to account for additional uptake.

Recent surface complexation models of uranyl sorption to smectites derived from fitting thermodynamic data from batch sorption reactions incorporate sorption of two aqueous uranyl species (monomeric UO_2^{2+}(aq) and polymeric $(UO_2)_3(OH)_5^+$) to three sites, the silanol (>SiOH) and aluminol (>AlOH) edge sites and exchange sites (X^-) (10–13). The sorption reactions that are modeled are based solely on the interactions of known or proposed uranyl solution species with these specific surface sites. Although the binding constants vary among these studies, all propose that high background electrolyte suppresses exchange and that the polymeric solution species do not sorb significantly at low pH and low uranyl solution concentrations. However, each of these studies proposes different stability constants for the surface species and thus predicts that different sets of species are important. Zachara and others (10–12) propose that the aluminol site is more reactive than the silanol site and that $>AlOUO_2^+$ is the predominant surface species over a broad range of pH values. However, the stability constant for $>AlOUO_2^+$ is lower in Turner *et al.*'s (12) model, and thus the mononuclear species, $>SiOUO_2^+$, is also significant at lower pH values. In contrast, Pabalan and Turner's (13) stability constants and model result in predictions that, while both of the mononuclear surface species are important, the $>SiOUO_2^+$ species is predominant. The smectite specimens differ among these studies, and this may account for some of the differences in the model predictions and derived parameters. In particular, the relative abundance of the different surface sites differs from material to material. Nonetheless, the discrepancies among these uranyl uptake and modeling studies underscore the need for independent information about the sorption complexes such as that derived from spectroscopic methods.

The existence of both exchange-site and edge-site surface complexes of uranyl species on montmorillonite has been experimentally demonstrated previously using molecular spectroscopic probes (31, 32). The present study combines systematic sorption experiments with several optical spectroscopic methods in the study of uranyl sorption complexes over a range of solution conditions. This study was undertaken to elucidate the role of varying solution chemistry on the nature of uranyl sorption species on montmorillonite using direct molecular spectroscopic probes.

MATERIALS AND METHODS

Materials

The reference montmorillonite, SAz-1 from Cheto, Arizona, was obtained from the University of Missouri Source Clay Repository; this material was used as received for the sorption experiments to facilitate comparisons with results from previous studies (31, 32). SAz-1 is a readily expandable, low [Fe], high cation exchange capacity (CEC ≈1.2 meq/g) montmorillonite with Ca^{2+} as the dominant interlayer cation and Na^+ comprising ≤5% of the total CEC; trace impurities of a silica phase have also been identified by infrared spectroscopy (33). Time-of-flight secondary ion mass spectrometric analysis (instrument in positive mode) of the as-received SAz-1 versus a peroxide and citrate/bicarbonate/dithionite-treated and Na^+-exchanged SAz-1 sample showed ≤0.1 wt% impurity Fe in the as-received material. Using the most conservative assumptions concerning the nature of this impurity (e.g., it is all contained within a cryptocrystalline goethite phase and all surface sites are available for uranyl sorption), it is estimated that this iron content could contribute at most 0.2 μmol/g SAz-1 to the sorption reactions (∼1 part in 6000 of the total exchange capacity). However, because of the conservative nature of the estimates used in this calculation, the actual contribution to sorption from impurity Fe is expected to be much lower.

Nitric acid, KNO_3, KOH, and $Ca(OH)_2$ solutions were prepared by diluting ACS reagent-grade solutions or solids in doubly deionized water. Uranyl solutions were prepared from recrystallized $UO_2(NO_3)_2 \cdot 6H_2O$ (Strem Chemicals) using doubly deionized water. pH and Ca^{2+} solution concentrations were determined with pH and ion-specific electrodes, respectively, using an Orion SA960 pH/ISE/mV meter. Uranium solution concentrations were determined spectrophotometrically using a modified Arsenazo-III method (34) or by inductively coupled plasma atomic emission spectrophotometry. Sorbed uranium concentrations were calculated as the difference between the initial and final uranium solution concentrations for the sorption experiments. Previous investigations have demonstrated that uranyl loss to reaction vessels is insignificant at the uranium concentrations employed in this study. Calcium release was calculated as the difference between the total solution concentration and that added during base addition to adjust pH.

Sorption Experimental Procedure

Sorption experiments were performed both in batch mode and as stepwise titrations. The batch-mode experiments were conducted in air at room temperature. For these experiments, SAz-1

was mixed end-over-end with a dilute HNO_3 solution (pH 3.5) for 32–40 h in a series of individual polyethylene tubes to fully hydrate the clay. Previous studies have shown that dissolution of SAz-1 is minimal at this pH (31, 32), and thus this pH was selected in order to have an initial pH value below that of complete adsorption and/or hydroxide precipitation. UO_2^{2+} was added to the suspensions as a nitrate solution and allowed to equilibrate for 2 to 4 h; pH was then adjusted to a range of values by adding varying amounts of 0.02 M $Ca(OH)_2$; the added Ca^{2+} was small compared to the initial calcium concentration derived from hydrating the clay. The final solids concentration was 20 g clay/L solution and total uranium concentration was 0.04 or 1.1 mM. The suspensions were then mixed end-over-end for 36–40 h, a period deemed sufficient for equilibration in independent tests. The suspensions were centrifuged, the final pH and Ca^{2+} concentration of the supernatant were measured, and aliquots of the supernatant were removed for uranium analysis.

Conditions for the titration experiments were comparable to those for the batch-mode sorption experiments. The titration experiments were specifically designed to monitor changes in dissolved calcium concentration in the SAz-1 suspensions as a function of pH in the presence and absence of uranium. Titration experiments were conducted in air in glass titration vessels; temperature was maintained at 20°C by circulating water through the jacket of the vessel. SAz-1 was mixed continuously with a dilute HNO_3 solution (pH ≈3.3) using a magnetic stir bar for ≈22 h. An aliquot of a uranyl solution or doubly deionized water was then added and the suspension allowed to equilibrate for an additional 2 to 3 h. The final solids concentration was 20 g/L; the final uranyl concentration was 0.04, 1.1, or 12.0 mM. The uranyl solution concentrations were selected to obtain a large range of surface coverages (<1 to ≈100% of the CEC for complete uptake). Base was added stepwise to the suspensions every ≈20 min; pH and Ca^{2+} concentration were measured just before each aliquot of base was added. The time between base additions (20 min) was selected to ensure completion of a well-defined titration curve without prolonged interruption (i.e., overnight); this step time allows for rapid reactions to occur but may not allow for the completion of slower reactions (see discussion under Results). The titrant was 0.02 M $Ca(OH)_2$ for suspensions with 0.04 or 1.1 mM UO_2^{2+} and 1 M KOH for 12.0 mM UO_2^{2+}. The higher molarity (unachievable with $Ca(OH)_2$ due to limited solubility) was necessary for the 12.0 mM UO_2^{2+} suspension to minimize the increase in volume of the suspensions during the titrations. Small aliquots of the suspensions were removed periodically and filtered for uranium analysis. In addition, titrations of suspensions of SAz-1 without uranyl were conducted with 0.02 M $Ca(OH)_2$ or 0.1 M KOH/0.9 M KNO_3.

Spectroscopic Measurements

Spectroscopic data were collected on both wet clay pastes and air-dried powder samples to assist in the identification of the differing sorption complexes (e.g., exchange vs edge sites). Wet paste samples were loaded into capped NMR tubes for data collection; these samples were then air-dried in the NMR tubes for data collection on parallel dry samples. Some samples were run only as air-dried powders. These were loaded into capillary tubes for spectroscopic studies.

Several different spectroscopic systems were employed to collect the data reported here. Continuous-wave (CW) emission spectra were obtained on a SPEX Industries Model 1403 scanning double monochromator equipped with 2400 g/mm holographic gratings, an RCA C31034 photomultiplier tube, and Stanford Research Model SR400 photon-counting electronics, or a SPEX Industries Fluorolog 2 System consisting of a Model 1681 single-stage 0.22-m excitation monochromator and a Model 1680 two-stage 0.22-m emission monochromator with a thermoelectrically cooled Hamamatsu Model R928 photomultiplier tube with photon-counting electronics. The excitation source in the former system was the 364- or 351-nm line from a Spectra Physics Model 2045 continuous-wave argon ion laser or the 407-nm line from a Spectra Physics Model 171 continuous-wave krypton laser. The excitation source in the latter system was a 450-W xenon arc lamp.

Time-resolved (TR) spectral data and lifetime measurements were collected on a system consisting of a Spectra Physics DCR-3G Nd:YAG pulsed laser, an Oriel Model 77250 1/8 m monochromator with a Hamamatsu R928 photomultiplier tube, a Stanford Research Systems Model SR445 fast preamplifier, and a Stanford Research Systems Model SR400 dual channel gated photon counter, or the Fluorolog 2 system described above equipped with a SPEX Industries Model 193D Phosphorimeter attachment. For the TR work with the former system the third harmonic of the Nd:YAG laser (355 nm) was used for excitation. The pulse width from this laser at 355 nm is ∼10 ns. For TR work with the latter system the flash-lamp unit provided with the Model 193D attachment was employed. The decay characteristics of the flash lamp prohibit investigation of processes occurring at less than ∼50 μs. For lifetime determinations with both systems, the gate-scanning capability of the photon counter was used.

Emission Spectroscopy: Background

The emissive electronic transitions in uranyl species can be described as ligand σ_u (axial oxygen 2*p* orbital)-to-metal δ_u (5*f* orbital) charge-transfer in nature (35–37). Even in fluid solutions at room temperature, the emission spectra of many uranyl species commonly exhibit a resolved vibronic structure. The structure derives from resolution of the vibrational energy levels in the ground electronic state associated with vibrational modes that are Franck–Condon active and/or have the appropriate symmetry to couple the ground- and excited-electronic states. By far the most important and frequently most pronounced mode is the totally symmetric stretch of the *trans*-dioxo moiety (O=U=O). In samples with multiple species, the resolution of these vibronic features degrades as the total spectral envelope consists of contributions from numerous uranyl species with differing zero-point electronic energies and vibronic spacings.

While the vibronic structure in the emission spectra of uranyl species appears to be the dominant feature, other important molecular structural factors contribute to the overall emission properties (spectral and temporal), thereby enhancing the speciation information that is encoded in the emission spectroscopic data. Among the more important factors are bonding modalities in the equatorial plane and longer range environmental effects (e.g., solvation). In aqueous solution, two important trends are discernible from the emission spectral data with increasing pH (and therefore increasing contributions from the uranyl hydrolysis products): (1) the entire spectral envelope shifts monotonically to lower energy and (2) the total intensity in the spectral envelope increases substantially (31, 38). The first effect is presumably the result of a shift to lower energy in the zero-point emission value(s) [$E_{0,0}$] of hydrolyzed uranyl species. Such shifts have also been observed for uranyl sorption species; Glinka *et al.* (39) argued that the zero-point energy value shifts to lower energies for chemically (as opposed to physically) sorbed uranyl on silica.

The measured excited-state lifetimes obtained from the emission decay data reflect the convolution of all processes (radiative, nonradiative, photochemical) that relax the electronic excited states back to the ground state. As previously noted, measured lifetimes are sensitive to the local coordination environment about the uranyl moiety. For example, the lifetimes of the hydrolyzed uranyl aqueous species are typically longer than that for the simple, fully hydrated uranyl species, UO_2^{2+} (38). Intrinsic electronic and molecular structural factors as well as environmental factors (wet vs dry samples, single crystal vs polycrystalline samples, variable temperatures, etc.) contribute to differing degrees to the measured lifetimes and make absolute comparisons of lifetime values difficult. However, trends in lifetime values for related samples have proved useful and are part of the data analyses used in the present report.

RESULTS

Sorption Experiments

The effect of pH on uranyl uptake is different for the three initial uranyl solution concentrations used in the batch uptake and titration experiments (Fig. 1). At the highest initial uranium solution concentration studied (12.0 mM), uptake was relatively constant from pH ≈3.0 to 4.2, above which uranium is rapidly removed and a yellowish precipitate formed.[3] For the two lower uranyl concentrations, uptake increases from its initial value to ~100% over 1–2 pH units, and the uptake curves for $[UO_2^{2+}]_{init} = 1.1$ mM are shifted to higher pH values than those for the lower uranyl concentration ($[UO_2^{2+}]_{init} = 0.04$ mM). The slope of the uptake curve for intermediate uranyl concentration

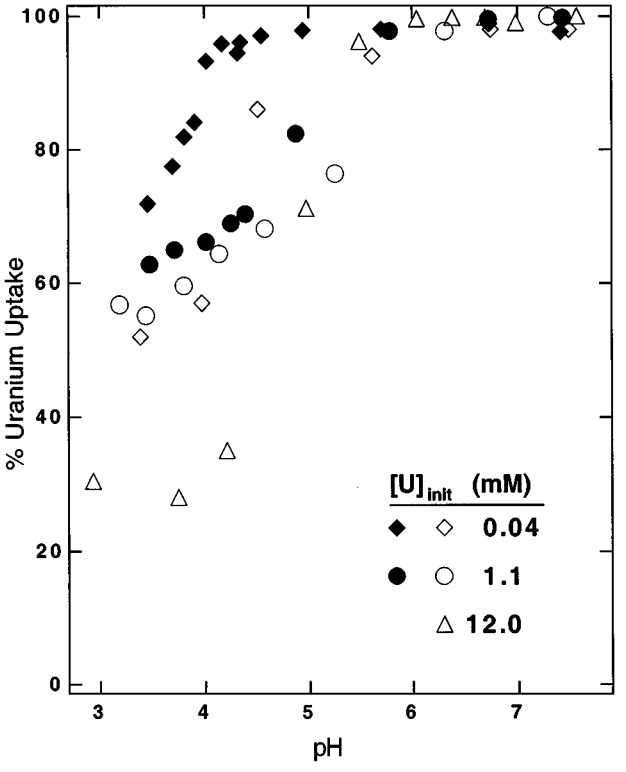

FIG. 1. Uranium uptake as a function of pH on Ca^{2+}–SAz-1. (open symbols, titration data; closed symbols, batch experiments).

(1.1 mM) is shallower than that for the low uranyl concentration, suggesting a combination of a relatively less pH-dependent and a more strongly pH-dependent uptake mechanism. Uranyl uptake in the titration experiments is less than that in the comparable batch experiments, which may indicate that equilibrium was not completely established in the shorter duration titration experiments.

The dominant uranyl solution species varies over the pH range and uranyl solution concentrations studied (Fig. 2). In general, uranyl becomes increasingly hydrolyzed and forms oligomeric solution species with increasing pH; these transitions occur at lower pH and to a greater extent for higher uranyl solution concentrations. Based on aqueous speciation calculations for the initial uranyl concentrations of this study, uranyl is predicted to occur predominantly as monomeric species at lower pHs (≥95% monomeric at pH ≤4.3 and 3.6 for low and moderate $[UO_2^{2+}]_{init}$, respectively). However, greater than 50% of the uranyl solution species are oligomeric, largely as the $(UO_2)_3(OH)_5^+$ species (Fig. 2), above pH ≈5.0 and 4.3 for the low and moderate $[UO_2^{2+}]_{init}$, respectively. These thermodynamic calculations also predict the formation of crystalline schoepite (hydrated uranyl oxide) at pH ≈5.6 and 4.6 for 0.04 and 1.1 mM uranyl solutions, respectively, although no precipitate was detected in either the low- or the moderate-coverage experiments. It is unlikely that crystalline schoepite will form in the short time allowed in the sorption experiments, and for the final uranyl concentrations of

[3] Because thermodynamic calculations predict the formation of uranyl hydroxide above pH ~4.2 in this experiment, further study of these conditions was not pursued in batch experiments.

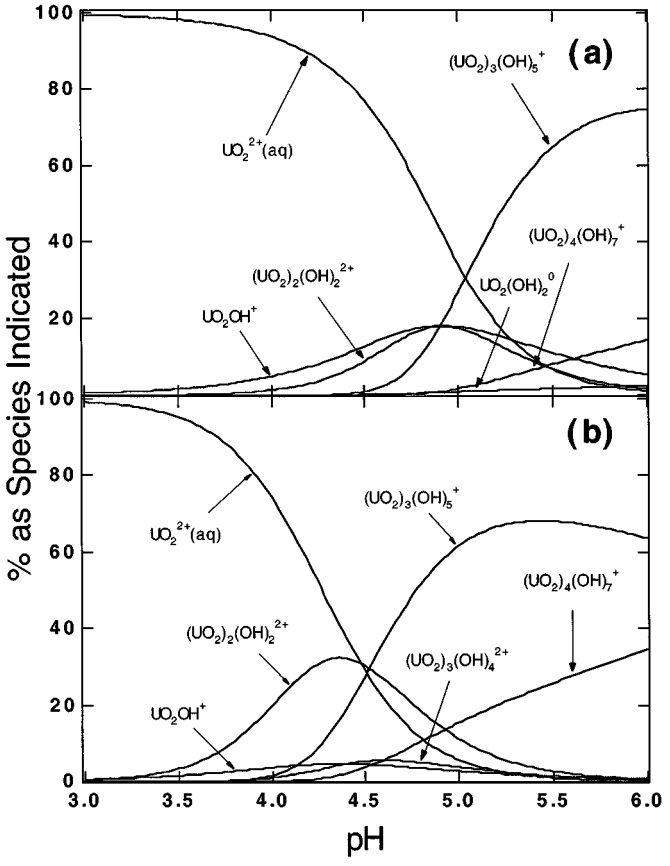

FIG. 2. Aqueous uranyl speciation diagrams, considering the initial uranyl and typical measured calcium solution concentrations for the batch sorption experiments: (a) Low-coverage samples: $[UO_2^{2+}]_{tot} = 0.04$ mM, $Ca_{tot} = 1.5$ mM, and (b) moderate-coverage samples $[UO_2^{2+}]_{tot} = 1.1$ mM, $[Ca^{2+}]_{tot} = 2.5$ mM. Speciation calculated using the computer program HYDRAQL (40); Uranyl equilibrium constants were taken from Grenthe (5) except as follows: $UO_2(OH)_2^0$ from (41); $UO_2(OH)_3^-$ and $(UO_2)_3(OH)_7^-$ from (42); crystalline and amorphous schoepite from (43); and becquerelite from (44). Solids were not allowed to precipitate in these calculations; over the pH range 3–6, crystalline schoepite is predicted to precipitate at pH ≈5.6 for (a), and crystalline schoepite, am-schoepite, and becquerelite are predicted to precipitate at pH ≈4.6, 5.3, and 5.5, respectively, for (b). The predicted pH for precipitation of amorphous schoepite is 7.8 and 5.8 for low and moderate coverages, respectively, if the initial uptake of uranyl is taken into account (i.e., assuming that the equilibrium solution concentrations are lower than the total added uranyl concentrations because of sorption).

the equilibrating solutions, no other solid (including amorphous uranyl hydroxide) is predicted to precipitate from solution at pH <5.8 for either the low or the moderate coverage experiments. Thus, the main change in uranyl species over the pH range studied is a shift from a predominance of uncomplexed, fully aquated uranyl $[UO_2^{2+}]$ to a mix of mainly oligomeric hydrolysis species (Fig. 2).

The Ca^{2+} displaced from the clay ($\Delta[Ca^{2+}]$) as a result of uranyl sorption processes was estimated in the titration experiments as the difference in dissolved $[Ca^{2+}]$ in samples containing uranium versus parallel samples that did not have added uranium, after first correcting for added Ca^{2+} from the base titrant. In several samples noted below $\Delta[Ca^{2+}]$ was negative, implying that more Ca^{2+} was released from the clay in the absence of uranium than when UO_2^{2+} species were present to compete for sorption sites. For titration experiments at the lowest $[U]_{init}$ (0.04 mM), $\Delta[Ca^{2+}]$ was ∼0 to slightly negative over the pH range 3.5 to 5.5. In contrast, for the intermediate and high $[U]_{init}$ samples, $\Delta[Ca^{2+}]$ was positive in the low-pH samples but again became slightly negative at the highest pH values. These results suggest that some calcium was displaced during uranium uptake at the moderate and high initial uranium concentrations. In fact, for $[U]_{init} = 12$ mM, $\Delta[Ca^{2+}]$ was approximately constant (0.20–0.23 mmol Ca^{2+}/g clay) over the pH interval 3.0 to 4.2 which corresponds closely to the measured UO_2^{2+} uptake (∼0.18 mmol/g clay). However, the presence of potassium (from the titrating base) precluded quantitative assessment of uranium/calcium exchange in this titration.

For the batch sorption reactions no parallel blank experiments (i.e., without added UO_2^{2+}) were conducted. Thus, the only measure of displaced Ca^{2+} as a result of UO_2^{2+} sorption processes was the equilibrium $[Ca^{2+}]$ value that also contains contributions from added $Ca(OH)_2$ for pH adjustment. These equilibrium $[Ca^{2+}]$ values ranged from 1.4 to 1.5 mM (0.07 to 0.075 mmol Ca^{2+}/g clay) for the 0.04 mM $[U]_{init}$ samples and 1.9 to 2.6 mM (0.095 to 0.13 mmol Ca^{2+}/g clay) for the 1.1 mM $[U]_{init}$ samples. Similar (but not precisely quantified) volumes of $Ca(OH)_2$ solution were required to adjust to a given pH in both the low and the intermediate $[U]_{init}$ samples, so these results do reflect a greater amount of displaced Ca^{2+} as a result of UO_2^{2+} sorption processes for the 1.1 mM samples than for the 0.04 mM samples. Viewed from a simpler mass balance perspective, the $[Ca^{2+}]/[UO_2^{2+}]$ ratio at equilibrium for the 0.04 mM $[U]_{init}$ samples was ∼35 versus ∼2 for the 1.1 mM $[U]_{init}$ samples. The large ratio in the former case likely suppresses UO_2^{2+} uptake into exchange sites (10–12).

Spectroscopic Data

Air-dried samples. The continuous-wave emission spectra for aqueous U(VI) sorbed on SAz-1 are characterized by prominent vibronic structure in the emission band. The spectra for uranyl sorbed from 0.04 mM U(VI) solution (resulting in coverages of 1.43 to 2.00 μmol/g) consist of a single dominant vibronic progression at all pH values for the air-dried samples (Fig. 3a). Note, however, that excitation by different wavelengths (351, 364, and 409 nm) yields slightly different luminescence spectra for uranyl at these low coverages (Fig. 3b). This excitation-wavelength-dependent behavior is observed for all samples in this low-coverage regime. In general, dependence of an emission spectrum on excitation wavelength suggests that more than one species is present in the sample. This provides the basis for synchronous excitation/emission scanning methods that are routinely used to unravel complex sample mixtures such as phosphorescent organic pesticides and fuels (45). Unfortunately, this synchronous scanning method is not applicable for much broader band emitters such as uranyl species.

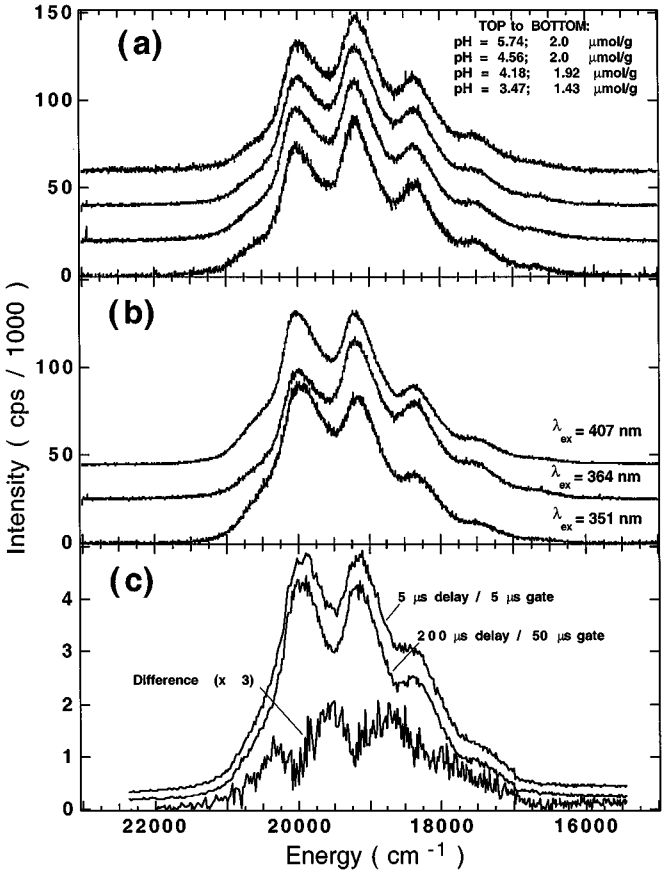

FIG. 3. (a) Changes in CW spectra ($\lambda_{ex} = 364$ nm) of sorption complexes as a function of pH at low coverage ($\Gamma = 1.43$–2.00 μmol/g). (b) Excitation wavelength dependence of CW spectra for sorbed uranyl at 2.0 μmol/g (pH 4.56). (c) Time-resolved spectra for uranyl sorbed to SAz-1 at low coverage (1.87 μmol/g, pH 4.0): (top) 5-μs delay/5-μs gate; (middle) 200-μs delay/50-μs gate; (bottom) difference spectrum.

The time-resolved emission and lifetime experiments also indicate the presence of multiple sorption species for the low-coverage samples. There are two distinct time-resolved spectra for the low-coverage sorption samples at all pH values studied (Fig. 3c); similarly, two distinct lifetimes can be resolved in the analysis of the emission decay data. The TR spectrum for longer gates and delays (which is dominated by the longer-lived "Species 1," S1) has a wider vibronic spacing than that seen in the spectrum for shorter gates/delays (corresponding to "Species 2," S2). This is direct evidence for the presence of multiple sorption species at these low coverages, as suggested by the excitation wavelength dependence of the CW spectra. Furthermore, the time-resolved spectra for a given gate/delay are quite similar for the different low-coverage sorption samples, indicating that the nature and distribution of the sorption species are similar at the different equilibrating pH values for these samples (i.e., each sample contains about the same relative concentration of species S1 and S2).

The CW emission spectra for uranyl sorbed from more concentrated solution (1.1 mM) show marked variation as a function of equilibrium pH and uranyl coverage (Fig. 4a). These results, and the excitation wavelength dependence of the CW emission spectra (Fig. 4b), indicate the presence of multiple, distinct sorption species at these coverages. The spectra at the low-coverage end of this series resemble those seen in all samples prepared from 0.04 mM UO_2^{2+}. At the higher coverage end of this series, however, the spectra become broad and poorly structured. The spectrum for uranyl hydroxide (Fig. 4b, inset) is also broad and lacks detailed vibronic structure, as seen for the highest pH sample under argon-ion laser excitation. However, the broadening of the features in the spectra for these moderate-coverage sorption samples is not necessarily due to the presence of a uranyl hydroxide precipitate, as the lifetimes for uranyl hydroxide are significantly longer (Table 1).

The time-resolved emission and lifetime experiments allow for further characterization of the sorption species present in the moderate-coverage samples. The short delay/narrow gate spectrum for the moderate-coverage sorption samples is poorly resolved (Fig. 4c). The long delay/wide gate spectrum for

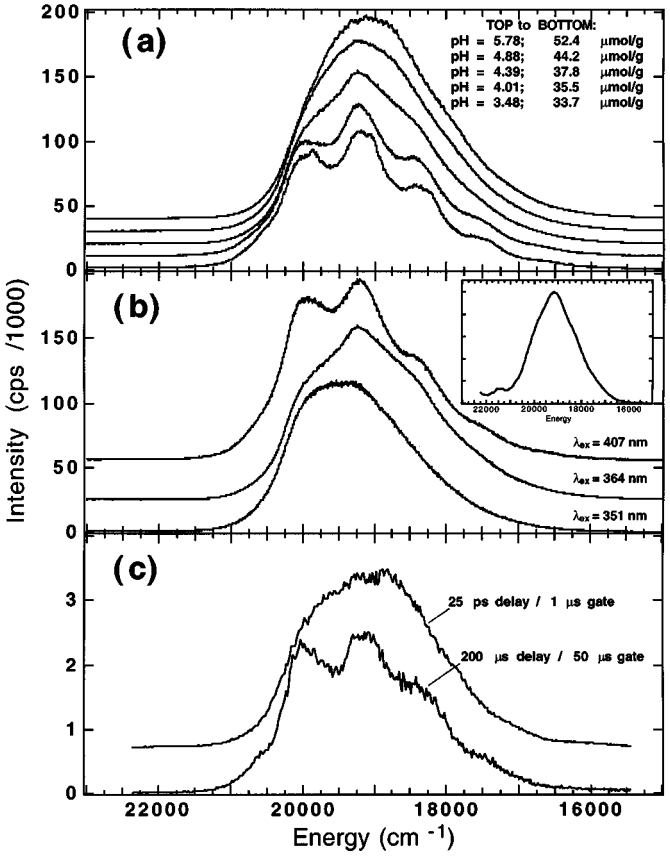

FIG. 4. (a) Changes in CW spectra ($\lambda_{ex} = 364$ nm) of sorption complexes as a function of pH at moderate coverage ($\Gamma = 33.7$–52.4 μmol/g). (b) Excitation wavelength dependence of CW spectra for sorbed uranyl at 37.8 μmol/g (pH 4.39). Inset is the CW emission spectrum for crystalline schoepite. (c) Time-resolved (TR) spectra for uranyl sorbed to montmorillonite at moderate coverages (37.8 μmol/g, pH 4.39): (top) 25 ps delay/1-μs gate; (bottom) 200-μs delay/50-μs gate.

TABLE 1
Summary of the Spectral Characteristics of Various Uranyl Species

Species	Lifetime (μs)	ΔE (cm^{-1})	$E_{0,0}$ (kcm^{-1})	Line width (description)
Uranyl sorption species				
S1[a]	170–270	820	20.00	Broad
S2[b]	2–12	740	20.25	Broad
S3[c]	15–25	nd	nd	Structureless
S4	80–110	820	19.85	Narrow
Uranyl aqueous species[d]				
UO_2^{2+}	<2	870	20.45	Narrow
$(UO_2)_3(OH)_5^+$	23	730	20.16	Broad
Uranyl hydroxide solids				
Fresh precipitate	63	nd	nd	Structureless
Aged precipitate	131	nd	nd	Structureless

[a] The variability in the lifetime for this prominent feature may in part reflect data truncation effects. Fits of the data were not improved by adding a second long lifetime.

[b] Fits of lifetime data for this component yield one or more short lifetimes; the multiple short lifetimes may reflect changes in the configuration of the surface complex.

[c] The spectrum for the S3 species is unstructured, centered at about ~19.2 kcm^{-1}; the $E_{0,0}$ and ΔE are not determined (nd). The lifetime appears to decrease upon drying the sample.

[d] From Moulin *et al.* (38) and this study.

moderate coverage is well-structured and resembles the long delay/wide gate spectrum for the low-coverage samples; however, the time delay necessary to obtain the resolved spectral component is greater for the moderate-coverage samples and increases with increasing coverage and pH. This indicates that the fractional population of the species that gives rise to this structured spectral component decreases relative to that of the broad, poorly structured component with increasing pH and coverage. Also, at least three distinct lifetimes are necessary to fit the emission decay curves; two lifetimes are similar to those obtained for the low-coverage samples and the third is intermediate between these two. Tentatively, this third lifetime (≈20 μs) is attributed to a new species ("Species 3," S3) that gives rise to the broad, poorly structured spectrum in Fig. 4c. Species 3 is present in all moderate samples, and the relative intensity of the S3 spectrum increases with increasing pH and coverage although the increase in intensity of this component does not appear to be linear with increasing coverage (Fig. 4). Although a very short lifetime consistent with species S2 is detected, the S2 spectrum cannot be resolved in these moderate-coverage samples through manipulations of the TR emission spectra.

Wet samples. Emission data were collected for four wet sorption samples: low coverage at pH 3.9 and 4.4 and moderate coverage at pH 3.7 and 4.2. These experimental conditions were intended to promote a dominant sorption mechanism, thereby focusing on a single type of sorption complex instead of the mixture observed at higher pH values. In particular, the moderate-coverage samples were expected to contain significant uranyl exchange-site complexes because of the low equilibrating pH, moderate uranyl concentrations, and low Ca/U ratio (≈2), whereas the sorption behavior as well as higher Ca/U ratio (≈35) for the low-coverage samples was expected to favor edge-site sorption (see, e.g., Ref. 11). Emission spectra were also collected for these samples after air-drying in order to assess changes in sorption complexes upon drying. As exchange complexes are thought to be fully hydrated, the greatest change was expected for these complexes; minimal change was expected for inner-sphere edge-site coordination complexes.

The emission spectra for most of the wet sorption samples show the emergence of a well-resolved, narrow-band spectrum (Fig. 5a). This feature (attributed to new "Species 4," or S4) is readily apparent in the moderate-coverage pH 3.7 and the low-coverage pH 4.4 samples and is detectable in the low-coverage pH 3.9 sample. The S4 component (including the corresponding lifetime) is lost upon drying (Fig. 5b), and the emission spectra of the dried samples resemble those of comparable samples in Figs. 3 and 4. In addition, subtraction of the S4 component from the wet sample CW spectra results in emission spectra very similar to those of the dried samples. As such, it appears that species S4 is the only identified sorption species that is present in wet samples but absent in dry samples. This spectral feature is isolated through manipulations of the CW and TR emission spectra. The spectrum has the same vibronic spacing and narrow bandwidth as that for aquated UO_2^{2+}, but the $E_{0,0}$ is shifted to

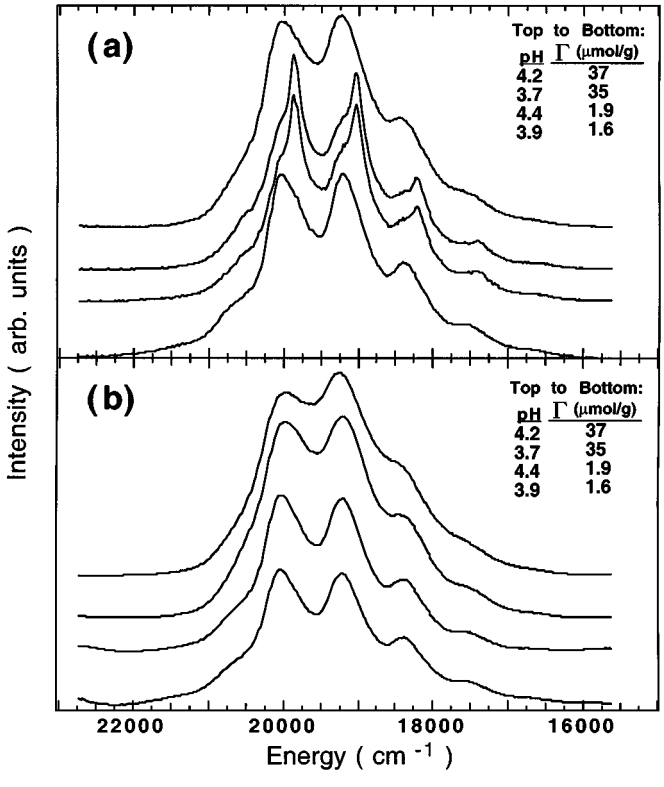

FIG. 5. Comparison of the CW emission spectra for (a) wet and (b) dried sorption samples.

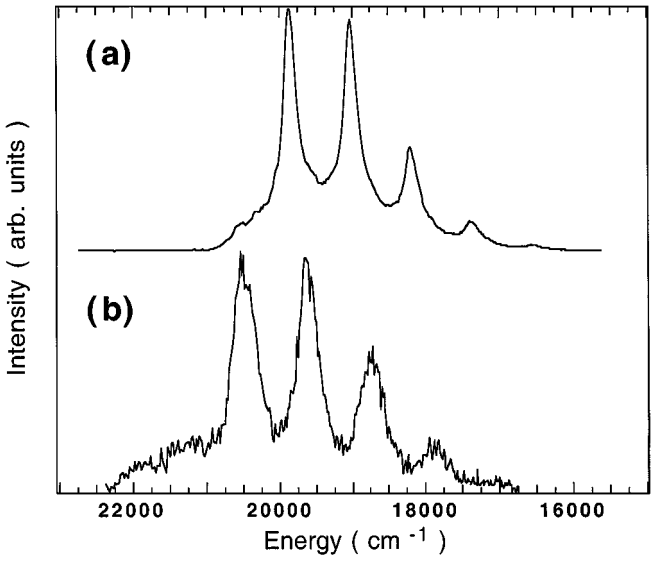

FIG. 6. Comparison of (a) the prominent spectral feature in several wet samples resolved from the spectra in Fig. 5(a) with (b) the spectra for fully aquated UO_2^{2+} (1 mM solution at pH ≈2).

lower energy (Fig. 6). In contrast, the spectrum for uranyl in exchange sites on wet sodium smectite (SWy-1) at similar pH (4.2) appears identical to the aqueous uranyl spectrum (Morris *et al.*, manuscript in preparation). The lifetime for S4 also is significantly longer (≈100 μs) than that of the aqueous species (<2 μs).

DISCUSSION

Results for the sorption and spectroscopic experiments provide strong evidence for the existence of several distinct uranyl sorption species on this calcium montmorillonite. The uptake curves for the titration and batch-mode experiments indicate that both pH-independent and pH-dependent processes may govern uranyl sorption under different solution conditions. Specifically, there is a narrow range (pH 3–4.2) of essentially pH-independent behavior observed in the 12.0 mM uranyl titration data that may reflect exchange processes. Similar behavior has been reported at low ionic strength and low pH for uranyl sorption on SWy-1 (11) and a smectitic soil isolate (12) and ascribed to an exchange mechanism. However, this exchange process may be suppressed by relatively high levels of background electrolyte, e.g., Ca/U ≥35 in the lowest uranyl concentration experiments (0.04 mM) reported here. The pH-dependent, strong sorption behavior for this low uranium concentration is consistent with a predominant mechanism of adsorption to amphoteric surface sites. Thus, the uptake experiments suggest that several sorption mechanisms are operating under different solution conditions, resulting in the formation of several different sorption species.

The optical spectroscopic data also provide strong evidence of multiple species; deconvolution of the CW spectra, excitation wavelength dependence of the CW spectra, multiple lifetimes, and distinct time-resolved spectra indicate the presence of multiple sorption species in these samples. At least four distinct sorption complexes may be identified (Table 1). The factors influencing the nature of the sorption species can be discerned by comparison of spectral data for these samples. Specifically, the roles of pH (which affects both uranyl solution speciation and surface site distributions), solution composition, and surface coverage may be examined.

Effect of Changes in Solution Speciation

The CW emission spectra for uranyl sorbed on SAz-1 from 0.04 mM solution over a range of equilibrium pH values are similar despite marked variations in uranyl solution speciation. In addition, the constancy of the CW and time-resolved spectra for these samples indicates that the two species (S1, S2) are present on the solid at a relatively constant ratio for the pH range studied. Based on thermodynamic calculations, the fully aquated monomeric UO_2^{2+} solution species comprises >98% of all uranyl species for a 0.04 mM uranyl solution at pH ≈3.48, whereas oligomeric uranyl species, in particular the $(UO_2)_3(OH)_5^+$ species, are predominant at pH ≈5.74 (Fig. 2). Thus, these spectroscopic data suggest that, at low surface coverages (≤2 μmol/g), the nature and distribution of the sorption complexes is not affected by the uranyl solution speciation. These results also suggest that the same, not necessarily dominant, solution species are the sorbing species over the entire pH range.

The emission spectra for uranyl sorbed on SAz-1 from 1.1 mM solution vary markedly as surface coverage increases (Fig. 4a). Based on the changes in relative peak intensities and positions of the CW spectra generated with different λ_{ex} and on deconvolution of the CW spectra, at least three distinct emission spectra can be detected. All three of these species may be detected in all of the moderate-coverage sorption samples, although their relative abundance varies as a function of surface coverage and pH. The existence of the same set of sorption species over widely varying equilibrium pH values again indicates that uranyl solution speciation does not influence the nature of the sorption species.

Changes upon Drying

Comparison of the data for the wet versus dry samples allows for determination of changes in sorption complexes upon drying and in this case provides evidence for a fourth type of sorption complex. The effects of drying the sorption samples vary among the different uranyl sorption species. Species 1 does not appear to be perturbed by drying. Changes in Species 2 were not detected, but this spectral component is less easily distinguished and analyzed because of its short lifetime and consequent minor contribution to the spectral domain data. The lifetime of Species 3 becomes slightly shorter upon drying, but the basic spectrum is not noticeably changed. In contrast, Species 4 disappears upon drying. This indicates that Species 4 is fully hydrated, retaining much of its aqueous character, as in an outer-sphere

complex. Because of the lack of data for higher pH wet samples, we cannot preclude formation of additional sorption complexes which lose their character upon drying; however, since the dry samples did not indicate the presence of new species at higher pH values, any such species are also likely to be weakly bound, outer-sphere complexes.

Availability of Binding Sites

One of the primary considerations in identifying the nature of a sorption complex is the availability of the different types of binding sites (amphoteric surface sites and exchange sites). Basal plane exchange-site densities can typically be estimated from measurements of the pH-independent contribution to the total cation exchange capacity. For example, for the Na^+-saturated smectite, SWy-1, McKinley *et al.* (11) found that the pH ~4 exchange capacity was approximately 0.6 mmol/g, but the CEC increased to ~0.75 mmol/g over the pH range from 4 to 10 from contributions from the amphoteric edge sites. Very similar relative abundances of pH-dependent and pH-independent exchange sites were reported for a smectitic soil isolate by Turner *et al.* (12). Uranyl isotherms on SAz-1 show a clear change in slope at ≈36–42 μmol/g (7, 32), which is equivalent to ~3% of the maximum CEC of SAz-1 (33). This suggests that the maximum edge-site capacity is about 40 μmol/g. This value lies between estimates of edge-site concentrations used in modeling uranyl sorption to montmorillonites. Typically, 10% of the external (N_2-BET) surface area is located at the clay edges (46), although tritium exchange measurements of site concentrations may be larger than those estimated from crystallite sizes (see, e.g., Ref. 12). Pabalan and Turner (13) modeled uranyl uptake on SAz-1 assuming that the average number of reactive sites on oxides (3.8 μmol sites/m^2, taken from Davis and Kent (47)) is a reasonable approximation for clay edges; this results in a total site density of ≈37 μmol/g for SAz-1. Others have modeled uranyl uptake on smectites assuming that the site density is equivalent to the total number of surface hydroxyls, based on crystallographic considerations (10, 11); this results in a surface site density (11.71 μmol sites/m^2) that is three times higher. However, the number of reactive surface sites is likely lower than this total surface hydroxyl value. Furthermore, aqueous uranyl species may occupy more than one surface site because they may be larger than a single surface site and/or form bidentate surface complexes under certain conditions, thereby occupying two surface sites (e.g., UO_2^{2+} sorption to ferrihydrite surface hydroxyl groups (22)). As such, the empirical data that suggest edge-site saturation at ≈36–42 μmol/g are reasonable. Thus, the three initial uranyl concentrations of 0.04, 1.1, and 12 mM could give rise to surface coverages that are well below ($\Gamma_{max} = 2$ μmol/g), near ($\Gamma_{max} = 55$ μmol/g), and greatly exceeding ($\Gamma_{max} = 600$ μmol/g) amphoteric surface site saturation, respectively.

The amphoteric surface sites consist of three distinct types: aluminol (>AlOH), silanol (>SiOH), and bridging (>Al–OH–Si<) groups. The latter are rarely considered in models of cation uptake, although their contribution has been inferred from detailed analyses of spectroscopic data (29). The theoretical ratio of aluminol to silanol groups on the edges of smectites is 0.83 (48). In general, the aluminol sites are considered much more reactive than the silanol sites, based on analogies to pure oxide phases, bond strength considerations, and simple modeling exercises. However, the acid–base properties of silanol and aluminol sites are different. While the overall isoelectric point for edges of smectites is pH ≈7–8 (49), the >SiOH groups are markedly more acidic; at lower pH values, the silanol groups will be primarily negatively charged whereas the aluminol sites will be positively charged. Therefore, there may be a difference in sorption behavior below aluminol site saturation (≈45% of total sites) as well as above and below total site saturation (≈36–42 μmol/g).

For exchange sites, both the abundance of sites and their selectivity influence exchange processes. The maximum coverage possible for the highest uranyl concentration (12 mM, titration data) is equivalent to the cation exchange capacity (≈exchange site population) of SAz-1. However, actual uptake did not exceed one-third of this before the onset of precipitation, and the moderate- and low-coverage samples were well below the total cation exchange capacity of SAz-1. Ca^{2+} is known to outcompete UO_2^{2+} for exchange sites in smectites (7, 12). As such, the high Ca/U ratio (≥35) for the low uranyl sorption samples may suppress exchange reactions. In contrast, for the moderate uranyl sorption samples, the Ca/U ratio is ≈2 and is less likely to inhibit exchange.

Proposed Assignments of Surface Species

The probable nature of the four sorption species may be inferred from consideration of the pH and coverages under which they form, changes in their relative abundance upon changes in equilibrium solution conditions, the availability of different types of surface sites, and specific spectral features (e.g., energies, vibronic spacings, vibronic band widths). Note, however, that absolute structural assignments are not possible based solely on the emission spectral data presented here, nor could they be easily derived from detailed X-ray absorption spectroscopy measurements given the presence of multicomponent surface complexation in these samples. The proposed structural assignments are based on emission data as well as wet chemical results and consideration of surface complexation theory to discern among alternative surface complexes. We offer these proposed structural assignments in part to provoke additional research, particularly combining spectroscopic measurements with detailed surface-complexation modeling to better constrain potential surface structural assignments (Morris *et al.*, manuscript in preparation).

Species 1 is a major component of emission spectra for all samples, wet or dry, high or low coverage (1.43–52.4 μmol/g), over the range of pH values studied (3.5–5.8). It is the dominant component of the CW spectra for the entire suite of

low-coverage samples. The corresponding uptake experiments ($[UO_2^{2+}]_{init} = 0.04$ mM) had a relatively high Ca : U ratio ($\geq$35) and show a strong pH dependence, which suggest binding to amphoteric surface sites. Previous EXAFS studies also demonstrated that the uranyl sorption complexes formed under similar solution conditions (pH $\approx$5.8, 10.3 μmol/g) undergo loss of coordinated water and/or hydroxide ions relative to fully aquated uranyl solution species (32). Last, the spectral character of this sorption complex does not change upon drying. Combined, these results are strong evidence that Species 1 is an inner-sphere sorption complex. The prevalence of Species 1 over a wide range of surface coverages proves that it is not representative of uranyl binding to a reactive trace impurity phase such as iron oxyhydroxide. Furthermore, a similar spectral signature has been observed for uranyl uptake onto purified, Na-saturated SWy-1 (Morris *et al.*, manuscript in preparation) under conditions that were satisfactorily modeled as sorption to >AlOH sites on the clay crystallite edges (11). Aluminol sites are generally considered more reactive than silanol sites. O'Day *et al.* (29) concluded that divalent cobalt formed bidentate surface complexes on adjacent aluminol (>AlOH) and bridging (>Al–OH–Si<) sites on kaolinite edges. By analogy, it is possible that Species 1 is a bidentate inner-sphere sorption complex bound to aluminol sites, some of which may be >Al–OH–Si< sites.

Species 2 forms under similar solution conditions as Species 1, yet several spectral characteristics of this complex suggest that it is an exchange-site complex and not a second inner-sphere sorption complex. Specifically, the much shorter emission lifetime and the shift of the spectral bands to higher energy for S2 imply that this surface species retains more coordinated water molecules as in exchange complexes. The exchange-site complex identified in our previous study (31) at much higher uranyl loading ($\sim$42% of CEC) also has similar spectral characteristics relative to those of the edge-site population. Furthermore, S2 forms at low pH values where exchange processes are favored. Models of uranyl sorption to smectites (11–13) do not propose formation of a second inner-sphere complex (e.g., $(UO_2)_3(OH)_5^+$ bound to silanol sites) until much higher pH values. Also, there is no evidence that polymeric solution species (e.g., $(UO_2)_3(OH)_5^+$) sorb to form inner-sphere complexes in this study. Both S1 and S2 form at low pH values where such polymeric solution species are present in only trace amounts (<0.1%, Fig.2). Furthermore, existing surface complexation model results predict a significant increase in the relative concentration of the polymeric sorption species with increasing pH, and yet there is no discernible pH dependence in the relative abundance of S1 and S2 at low coverages.[4] Any increase in the ratio of inner-sphere to exchange complexes over pH $\approx$3.5 to 5.8 is expected to be much less than that predicted for the ratio of polymeric to monomeric inner-sphere complexes. As such, the minimal variation in the S1/S2 suggests that S2 likely is an exchange complex. Note, though, that without the ability to better quantify the S1/S2 ratio, we cannot discount that there may an alternative, as of yet undefined, explanation for the spectral characteristics of Species 2, particularly if the S1/S2 ratio is constant.

Species 2 is distinct from the exchange complex formed on a sodium smectite (SWy-1; Morris *et al.*, manuscript in preparation). The spectrum for uranyl at exchange sites on Na^+–SWy-1 is virtually indistinguishable from that for fully aquated UO_2^{2+}; in contrast, the peaks are markedly broader and the peak separation much smaller for Species 2, although the lifetime and $E_{0,0}$ value are similar to those for the exchange site population on SWy-1. Furthermore, the spectrum for Species 2 did not appear to change upon drying, but the signal was lost for the exchange-site complex on Na–SWy-1 in dried samples. These differences may be due in part to differences between the two smectites: SAz-1 is a calcium montmorillonite with minimal to no tetrahedral substitution whereas the SWy-1 studied is a sodium smectite with partial tetrahedral substitution. The extent of tetrahedral substitution affects the local charge environment of the exchange sites and binding strength of the interlayer cations. Moreover, sodium smectites readily expand upon wetting and may become fully dispersed, allowing for a more aqueous-like interlayer. The interlayer of calcium smectites only slightly expands (doubling interlayer water) upon wetting, resulting in a more constricted environment. Thus the exchange sites in Ca^{2+}–SAz-1 and Na^+–SWy-1 are expected to differ, especially for the wet clays.

The structureless spectrum ascribed to Species 3 is detected in all moderate coverage samples, increasing in abundance with increasing coverage. At these moderate coverages, aluminol sites are near or above saturation, especially if uranyl bonds in a bidentate fashion. Species 3 is thought to be a polymeric surface complex, possibly anchored to the surface by interaction with uranyl previously sorbed to aluminol sites (i.e., Species 1). The spectrum for Species 3 resembles that of schoepite (Fig. 4b, inset), although the shorter lifetime and shift in energy suggest that it is not a well-crystallized precipitate. Furthermore, S3 forms in solutions (e.g., at pH 3.5) that are undersaturated with respect to uranyl hydroxide by more than one order of magnitude. However, the similarity between the spectra for S3 and uranyl hydroxide could be indicative of the formation of a hydroxide-like planar polymeric species as seen for other sorbed metals on oxides and clays (27–30) or a poorly crystallized hydroxide-like phase (50, 51). Furthermore, the absolute emission intensity attributed to S3 does not increase linearly with increasing coverage. In simple systems at low concentrations of emitting species, the emission intensity should increase linearly with increasing concentration of the emitting species (52, 53). Nonlinear behavior arises from the self-quenching processes and is frequently observed in systems of large aggregates and/or high local concentrations of emitting species. Thus, the spectral characteristics of Species 3 are consistent with the growth of polymeric uranyl surface complexes on montmorillonite with increasing surface coverages.

[4] While the short lifetime of S2 renders detection and quantification of this species challenging, the S1/S2 ratio can only be slightly changing or nearly invariant to be consistent with the observed spectral features.

Species 4 is distinguished by its prominent, narrow-band vibronic structure and is seen in only a subset of the wet sorption samples. The disappearance of its spectral signature upon drying suggests that it may be an outer-sphere complex in which the uranyl species interacts electrostatically with the surface as an ion-pair complex. This spectrum loosely resembles that for fully aquated UO_2^{2+}, suggesting that it, too, might be fully aquated. However, the $E_{0,0}$ for S4 is red-shifted, and the lifetime is considerably longer, indicating some perturbation of the fully aquated coordination environment. Moulin *et al.* (38) found that the spectrum for the first hydrolysis product of uranyl in aqueous solution $[UO_2(OH)^+]$ is similarly red-shifted from that of the fully aquated monomer, and the measured emission lifetime for this hydrolysis species is greatly increased ($\approx$80 μs). While caution must be exercised when comparing distinctly different bonding environments because the inferences of bond strength depend on a knowledge of the symmetry of the sorption complex (39), the similarities between the hydrolyzed aqueous species $UO_2(OH)^+$ and Species 4 suggest that S4 might also be a minimally hydrolyzed species. However, the other evidence still suggests an outer-sphere complex of such a species. Formation of outer-sphere sorption complexes on kaolinite has been inferred from the ionic strength dependence of metal-ion uptake (29). Such complexes were found to form at lower pH values on certain kaolinites, with inner-sphere complexation dominating at higher pH values and coverages. Thus it is not surprising that outer-sphere complexes can form on montmorillonite at lower pH values.

SUMMARY

Four distinct uranyl sorption complexes on montmorillonite have been identified spectroscopically and may coexist under certain conditions. Most notable is the preponderance and persistence of an inner-sphere sorption complex over a range of solution conditions and coverages. The inner-sphere complex (Species 1) does not appear to be affected by drying of the clay. There is also evidence that an exchange complex (Species 2) forms under these conditions, although assignment of this species is equivocal. This putative exchange-site complex (Species 2) is distinct from that on sodium SWy-1. These results are consistent with recent models of uranyl uptake (10, 11) which included inner-sphere complexation to aluminol sites and formation of exchange complexes by monomeric UO_2^{2+}. An outer-sphere complex also forms under certain solution conditions that may be minimally hydrolyzed. In contrast with the inner-sphere and exchange-site complexes, the spectral signature of outer-sphere complexes is lost upon drying, further substantiating the weak surface bond of such complexes. Uranyl also is shown to form polymeric inner-sphere complexes at moderate coverages. The relatively high Ca^{2+} solution concentrations and the Ca : U competition for exchange sites may favor the formation of such species over exchange complexes as the site occupancy for the amphoteric edge sites is approached. Despite the presence of up to four distinct surface species under certain equilibrating conditions, it does not appear that a variety of different solution species are interacting with the solid. Rather, the data suggest that the fully aquated uranyl species is likely the principal solution species interacting with the solid to form all four types of sorption complexes over the range of solution conditions (uranyl concentrations and pH) studied herein. These spectroscopic results allow for refinement of surface complexation models of uranyl sorption to smectites, which must account for the different relative strengths and abundances of the four distinct surface complexes.

ACKNOWLEDGMENTS

This work was supported by the Subsurface Science Program of the Office of Biological and Environmental Research, Office of Science, of the United States Department of Energy and by the Laboratory-Directed Research and Development program at Los Alamos National Laboratory. The authors express their gratitude to Ms. Robin Richard for experimental assistance.

REFERENCES

1. Riley, R. G., and Zachara, J. M., "Chemical Contaminants on DOE Lands and Selection of Contaminant Mixtures for Subsurface Science Research," DOE/ER-0547T. Washington, DC. U.S. Department of Energy, Office of Energy Research, 1992.
2. Bernhard, B., Geipel, G., Brendler, V., and Nitsche, H., *J. Alloys Compounds* **271–3**, 201 (1998).
3. Abdessalam, A., Lutze, W., and Nuttall, H. E., *in* "Uranium: Mineralogy, Geochemistry and the Environment" (P. C. Burns and R. Finch, Eds.), p. 433. Mineralogical Society of America, Washington, 1999.
4. Weigel, F., *in* "Chemistry of the Actinide Elements" (J. J. Katz, G. T. Seaborg, and L. R. Morss, Eds.), Ch. 5., Chapman & Hall, New York, 1986.
5. Grenthe, I., "Chemical Thermodynamics of Uranium." North-Holland, New York, 1992.
6. Borovec, Z., *Chem. Geol.* **32,** 45 (1981).
7. Tsunashima, A., Brindley, G. W., and Bastovanov, M., *Clays Clay Mins.* **29,** 10 (1981).
8. Ames, L. L., McGarrah, J. E., Walker, B. A., and Salter, P. F., *Chem. Geol.* **35,** 205 (1982).
9. Ames, L. L., McGarrah, J. E., and Walker, B. A., *Clays Clay Mins.* **31,** 321 (1983).
10. Zachara, J. M., and McKinley, J. P., *Aquat. Chem.* **55,** 250 (1993).
11. McKinley, J. P., Zachara, J. M., Smith, S. C., and Turner, G. D., *Clays Clay Min.* **43,** 586 (1995).
12. Turner, G. D., Zachara, J. M., McKinley, J. P., and Smith, S. C., *Geochim. Cosmochim. Acta* **60,** 3399 (1996).
13. Pabalan, R. T., and Turner, D. R., *Aquat. Geochem.* **2:203** (1997).
14. Jaffrezic-Renault, N., Poirier-Ansrade, H., and Trang, D. H., *J. Chromatogr.* **201,** 187 (1980).
15. Yamashita, H., Ozawa, Y., Nakajima, F., and Murata, T., *Bull. Chem. Soc. Japan* **53,** 1 (1980).
16. Maya, L., *Radiochim. Acta* **31,** 147 (1982).
17. Tripathi, V. J., "Uranium(VI) Transport Modeling: Geochemical Data and Submodels." Ph.D. Dissertation, Stanford University, 1984.
18. Hsi, C.-K. D., Langmuir, D., *Geochim. Cosmochim. Acta* **49,** 1931 (1985).
19. Ho, C. H., and Doern, D. C., *Can. J. Chem.* **63,** 1100 (1985).
20. Ho, C. H., and Miller, N. H., *J. Colloid Interface Sci.* **106,** 281 (1985).
21. Ho, C. H., and Miller, N. H., *J. Colloid Interface Sci.* **110,** 165 (1986).
22. Waite, T. D., Davis, J. A., Payne, T. E., Waychunas, G. A., and Xu, N., *Geochim. Cosmochim. Acta* **58,** 5465 (1994).

23. Maes, A., Peigneur, P., and Cremers, A., *Proc. Int. Clay Conf.* 1975, 319 (1976).
24. Stumm, W., Hohl, H., and Dalang, F., *Croatica Chem. Acta* **48,** 491 (1976).
25. Schindler, P. W., *in* "Adsorption of Inorganics at Solid–Liquid Interfaces" (M. A. Anderson and A. J. Rubin, Eds.) p. 1. Ann Arbor Science, Ann Arbor, MI, 1981.
26. Sposito, G., "The Surface Chemistry of Soils." Oxford Univ. Press, New York, 1984.
27. Chisholm-Brause, C. J., O'Day, P. A., Brown, G. E., and Parks, G. A., *Nature* **348,** 528 (1990).
28. Katz, L. E., and Hayes, K. F., *J. Colloid Interface Sci.* **170,** 491 (1995).
29. O'Day, P. A., Parks, G. A., and Brown, G. E., Jr., *Clays Clay Min.* **42,** 337 (1994).
30. O'Day, P. A., Chisholm-Brause, C. J., Towle, S., Parks, G. A., and Brown, G. E., Jr., *Geochim. Cosmochim. Acta* **60,** 2515 (1996).
31. Morris, D. E., Chisholm-Brause, C. J., Barr, M. E., Conradson, S. D., and Eller, P. G., *Geochim. Cosmochim. Acta* **58,** 3613 (1994).
32. Chisholm-Brause, C. J., Conradson, S. D., Buscher, C. T., Eller, P. G., and Morris, D. E., *Geochim. Cosmochim. Acta* **58,** 3625 (1994).
33. Van Olphen, H., and Fripiat, J. J., "Data Handbook for Clay Materials and Other Non-metallic Minerals." Pergamon Press, New York, 1979.
34. Savvin, S. V, *Talanta* **8,** 673 (1961).
35. McGlynn, S. P., Smith, J. K., and Neely, W. C., *J. Chem. Phys.* **35,** 105 (1961).
36. Bell, J. T., and Biggers, R. E., *J. Mol. Spectrosc.* **22,** 262 (1967).
37. Denning, R. G., *Structure Bonding* **79,** 214 (1992).
38. Moulin, C., Laszak, I., Moulin, V., and Tondre, C., *Appl. Spectrosc.* **52,** 528 (1998).
39. Glinka, Y. D., Jaroniec, M., and Rozenbaum, V. M., *J. Colloid Interface Sci.* **194,** 455 (1997).
40. Papelis, C., Hayes, K. F., and Leckie, J. O., "HYDRAQL: A Program for the Computation of Chemical Equilibrium Composition of Aqueous Batch Systems Including Surface-Complexation Modeling of Ion Adsorption at the Oxide/Solution Interface." Stanford University Technical Report No. 306, 1988.
41. Silva, R. J. *Mat. Res. Soc. Symp. Proc.* **257,** 323 (1992).
42. Sandino, M. C. A., and Bruno, J., *Geochim. Cosmochim. Acta* **56,** 4135 (1992).
43. Torrero, M. E., Casas, I., dePablo, J., Sandino, M. C. A., and Grambow, B., *Radiochim. Acta* **66/67,** 29 (1994).
44. Sandino, M. C. A., and Grambow, B., *Radiochim. Acta* **66/67,** 37 (1994).
45. Hofstraat, J. W., and Wild, U. P., *J. Fluoresc.* **8,** 319 (1998).
46. Wanner, H., Albinsson, Y., Karnl, O., Wieland, E., Wersin, P., and Charlet, L., *Radiochim. Acta* **66/67,** 733 (1994).
47. Davis, J. A., and Kent, D. B., *in* "Mineral–Water Interface Geochemistry" (M. F. Hochella and A. F. White, Eds.), p. 177. Mineralogical Society of America, Washington, 1990.
48. White, G. N., and Zalazny, L. W., *Clays Clay Min.* **36,** 141 (1988).
49. Kraepiel, A. M., Keller, K., and Morel, F. M. M., *Environ. Sci. Tech.* **32,** 2829 (1998).
50. Farley, K. J., Dzombak, D. A., and Morel, F. M. M., *J. Colloid Interface Sci.* **106,** 226 (1985).
51. Steefel, C. I., and Van Cappellen, P., *Geochim. Cosmochim. Acta* **54,** 2657 (1990).
52. Benson, P., Cox, A., Kemp, T. J., and Sultana, Q., *Chem. Phys. Lett.* **35,** 195 (1975).
53. Burrows, H. D., Cardoso, A. C., Formosinho, S. J., and Miguel, M. D. M., *J. Chem. Soc. Faraday Trans.* **81,** 49 (1985).